Structural Polymorphism of Poly(ethylene oxide)−Poly(propylene oxide) Block Copolymers in Nonaqueous Polar Solvents

Paschalis Alexandridis*

Department of Chemical Engineering, University at Buffalo, State University of New York, Buffalo, New York 14260-4200

Received May 12, 1998; Revised Manuscript Received July 13, 1998

ABSTRACT: The solution properties of water-soluble amphiphiles in nonaqueous polar solvents are important in the elucidation of the effects of solvent quality on self-assembly and also in practical applications where the use of water as a solvent is undesirable. We studied the self-assembly of a poly(ethylene oxide)−poly(propylene oxide) (PEO−PPO) block copolymer (Pluronic P105: $EO_{37}PO_{58}EO_{37}$) in formamide (as selective solvent for the PEO block) and present here results on the binary concentration−temperature phase diagram and on the microstructure. In addition to formamide-rich and polymer-rich solution regions, four "gel" regions with different microstructures, stable over a wide temperature range (from 20 °C to more than 90 °C), have been identified and characterized by small-angle X-ray scattering (SAXS). The PEO−PPO block copolymer in formamide exhibits a thermoreversible transition from a micellar solution to a micellar cubic gel (of *Pm*3*n* crystallographic structure) at 25−35 wt % polymer concentrations. At higher polymer concentrations, regions with hexagonal (cylindrical), bicontinuous cubic, and lamellar (smectic) lyotropic liquid crystalline microstructures are stable. The formation of the bicontinuous cubic structure (consistent with the *Ia*3*d* crystallographic space group and the gyroid minimal surface) in formamide is notable, given the rarity of such structure in PEO−PPO block copolymer−water systems. The change of solvent from water to formamide did not diminish the structural polymorphism of the PEO−PPO block copolymer. However, the stability regions of the different structures (and in particular of the micellar cubic) in the case of formamide are shifted to higher polymer concentrations and temperatures compared to water. These observations can be related to a higher solubility of both PEO and PPO in formamide compared to water, and a higher effective PEO/PPO block ratio of the polymer. The interfacial area-per-polymer values (extracted from SAXS data) in the lamellar and hexagonal structures are 10% and 20% higher, respectively, in the case of formamide than in water, in corroboration with the phase behavior observations.

Introduction

Amphiphiles (molecules consisting of parts having different chemical nature) find widespread applications because of their unique ability to self-assemble and modify interfacial properties.[1] Surfactants are well-known to form thermodynamically stable assemblies in aqueous solutions.[2] Block copolymers also express amphiphilic character and can attain a number of microstructures, such as lamellae, cylinders, and spheres, in the absence of solvent or in mixtures with homopolymers.[3] The self-assembly of block copolymers in solution, and in particular in water, is attracting considerable attention.[4−6]

Amphiphilic block copolymers consisting of water-soluble poly(ethylene oxide) (PEO) and water-insoluble poly(propylene oxide) (PPO) blocks are commercially available as Poloxamers or Pluronics in the 2000−20000 molecular weight range and 20−80 wt % PEO content range.[7] The versatility of the PEO−PPO copolymers in numerous practical applications emanates (i) from the broad and controllable range of amphiphilic properties achieved by the variation of the block copolymer hydrophobe−hydrophile composition and total molecular weight and also (ii) from the sensitivity of their aqueous solution properties to the temperature (this is due to the worsening with increasing temperature of the water solvent quality with respect to both PEO and PPO).[7] PEO−PPO block copolymers in aqueous solutions can self-assemble into spherical micelles (with a PPO core and a hydrated PEO corona), above a certain polymer concentration, CMC (critical micellization concentration), and above a certain solution temperature, CMT (critical micellization temperature), which depend on the PEO/PPO ratio and polymer molecular weight.[8] The formation of thermoreversible "gels" is a notable self-assembly feature of PEO−PPO block copolymers in water. Such gels have been known for long time[9] and utilized in, e.g., controlled release,[10] but their structure has only recently been resolved and related to lyotropic liquid crystalline organization based on self-assembly.[11−13]

Significant advances have been made over the recent years on (i) the identification of different morphologies (e.g., cubic, hexagonal, and lamellar) attained by PEO−PPO block copolymers in binary systems with water (selective solvent for PEO) and also in ternary systems with water and an organic solvent selective for PPO, (ii) the delineation of the composition−temperature ranges where various morphologies occur (phase behavior), and (iii) their structural characterization using primarily small-angle X-ray and neutron scattering techniques.[11,12,14] PEO−PPO block copolymers are remarkable in that they can form the whole spectrum of self-assembled structures, from micellar solutions in water, to lyotropic liquid crystals (of "oil-in-water" or "water-in-oil" topology, and including bicontinuous cubic structures), to water-swollen micelles in organic solvents.[12,15] Such work establishes PEO−PPO block copolymers as a model system for the study of phase behavior, microstructure, and dynamics of block copoly-

* E-mail: palexand@eng.buffalo.edu. Fax: (716) 645 3822.

S0024-9297(98)00752-9 CCC: $15.00
Published on Web 09/12/1998

mers in the presence of selective solvents, and a link between the phase behavior of surfactants in solution and that of solvent-free block copolymers. It also corroborates De Gennes' foresight that "block copolymers can give us the best model of amphiphilic behavior".[16]

The structural polymorphism of PEO−PPO block copolymers has been connected to the relative swelling of the macromolecular PEO and PPO blocks by the low-molecular weight solvent molecules.[15] The solvent quality is thus a controlling factor of the block copolymer self-assembly. While a number of solvents selective for the PPO block have been tested,[17] water is the only selective solvent used so far for the PEO block. The solvent quality of water toward PEO and PPO can be altered by a change in temperature or by the addition of cosolutes such as alcohols[18] or salts;[19] however, it is desirable to replace water completely by a nonaqueous polar solvent for some applications.

The elucidation of the phase behavior and structure of amphiphiles in nonaqueous solvents is important (i) fundamentally for a description of the "hydrophobic effect" (which is considered responsible for the self-assembly of amphiphiles in water)[20] and (ii) for practical applications in which the presence of water is undesirable because of, for example, the possibility of corrosion.[21] These considerations have motivated a number of studies on the solution behavior of surfactants in a variety of nonaqueous polar solvents, e.g., hydrazine, formamide, *N*-methylformamide, glycerol, propylene glycol, and ethylene glycol.[22] Formamide ($HCONH_2$) has been the solvent studied most extensively in this context.[23−25] Nonionic PEO−alkyl ether surfactants have been found to form micelles and even lyotropic liquid crystalline structures in formamide, but over different conditions than in water.[23] Cloud point (macrophase separation) measurements for a PEO−PPO block copolymer in formamide have been made[26] and a report on the synthesis of ordered macroporous materials by templating with oil-in-formamide emulsions stabilized by PEO−PPO−PEO block copolymers has appeared very recently.[27] To the best of our knowledge, no one has reported an explicit examination of the self-assembly of PEO−PPO block copolymers in nonaqueous polar solvents.

We thus selected formamide as a nonaqueous polar solvent, and set out to study the phase behavior and structure in formamide of a PEO−PPO block copolymer with known aqueous self-assembly properties.[28,29] We report here the phase diagram of $EO_{37}PO_{58}EO_{37}$ (Pluronic P105) in formamide, over the whole concentration range and the 5−90 °C temperature range. We have identified six regions of different microstructures. We present evidence (from small-angle X-ray scattering, SAXS)) on the structure in the various "gel" regions, in the order of increasing polymer concentration. We then compare and contrast the PEO−PPO self-assembly in formamide and in water, and also compare the PEO−PPO−solvent systems to those of nonionic PEO−alkyl ether surfactants.[23,30]

Materials and Methods

Materials. The Pluronic P105 poly(ethylene oxide)-*block*-poly(propylene oxide)-*block*-poly(ethylene oxide) copolymer was obtained as a gift from BASF Corp. and was used as received. P105 can be represented by the formula $(EO)_{37}(PO)_{58}(EO)_{37}$ on the basis of its nominal molecular weight of 6500 and 50% PEO content. Formamide ($HCONH_2$) was purchased from Fluka Chemie AG, Buchs, Switzerland. Care was taken to avoid exposure of formamide to atmospheric humidity. Samples were prepared individually by weighing appropriate amounts of polymer and formamide into 8 mm (i.d.) glass tubes, which were immediately flame-sealed. The samples were centrifuged repeatedly in alternating directions over the course of several days to facilitate homogenization. During this time period, the samples were kept at 25 ± 0.5 °C. Subsequently, the samples were left at a given temperature in a temperature-controlled bath or oven for several days at a time, to attain equilibrium at this temperature. Following the equilibration period, the samples were checked for phase separation (1-phase samples were clear and macroscopically homogeneous; the 2-phase samples either were homogeneous but opaque or were macroscopically heterogeneous/phase-separated) and optical anisotropy under polarized light (micellar solutions or cubic lyotropic liquid crystals are isotropic/nonbirefringent, while lamellar or hexagonal lyotropic liquid crystals are anisotropic/birefringent). The visual distinction between one- and two-phase samples is less clear in the formamide system than it is in water but is adequate and is abetted by the fact that the optically isotropic (micellar solution, L_1; micellar cubic, I_1; bicontinuous cubic, V_1) and optically anisotropic/birefringent (hexagonal, H_1; lamellar, L_α) regions alternate (see Figure 1) and is easy under polarized light to discern an optically isotropic from a birefringent sample. As to the visual distinction between isotropic solution (L_1) and isotropic cubic (I_1) phases, there is a discernible meniscus, but more importantly, the isotropic solution can flow, whereas the cubic phase cannot, thus allowing for an easy distinction between the two.

Small-Angle X-ray Scattering (SAXS). SAXS measurements were performed on a Kratky compact small-angle system equipped with a position sensitive detector (see refs 12 and 29 for details). The obtained Bragg diffraction peaks are relatively sharp, in which case the correct peak position can be evaluated directly from the slit-smeared data.[12,29] The structure of the lyotropic liquid crystalline phases was determined from the relative positions of the SAXS diffraction peaks. For the lamellar (smectic) and hexagonal (cylindrical assemblies crystallized in a two-dimensional hexagonal lattice) structures, the position of the peaks should obey the relationships 1:2:3:... and $1:\sqrt{3}:2:\sqrt{7}:3...$, respectively. The lattice parameters d (lamellar periodicity) and a (distance between the centers of adjacent cylinders) of the lamellar and hexagonal structures, respectively, were obtained from the position (q^*) of the first (and most intense) diffraction peak:

$$\text{lamellar:} \quad q^* = \frac{2\pi}{d} \qquad \text{hexagonal:} \quad q^* = \frac{4\pi}{a\sqrt{3}} \tag{1}$$

The thickness of the apolar domains, δ, in the lamellar structure and the radius of the apolar domains, R, in the hexagonal structure were calculated from the lattice parameters and the volume fraction, f, of the apolar (PPO) components in the binary system (see ref 12 for more details on the definition of "polar" and "apolar" domains):

$$\text{lamellar:} \quad \delta = df \qquad \text{hexagonal:} \quad R = a\left(\frac{\sqrt{3}}{2\pi f}\right)^{1/2} \tag{2}$$

In the lamellar structure, the effective area per PEO block at the interface between polar and apolar domains (interfacial area, α_p) can be determined from the lattice parameters without any assumptions concerning the degree of segregation or the local structure of the copolymer film.[12,29] The calculation of α_p in the hexagonal structure involved the assumption that the apolar domains consist of all the PPO in the system (v_p is the volume of one P105 polymer molecule, $v_p \approx 10\,300$ Å^3; Φ_p is the polymer volume fraction).

$$\text{lamellar:} \quad \alpha_p = \frac{v_p}{d\Phi_p}$$

$$\text{hexagonal:} \quad \alpha_p = \frac{v_p}{a\Phi_p}\left(\frac{2\pi}{\sqrt{3}f}\right)^{1/2} \tag{3}$$

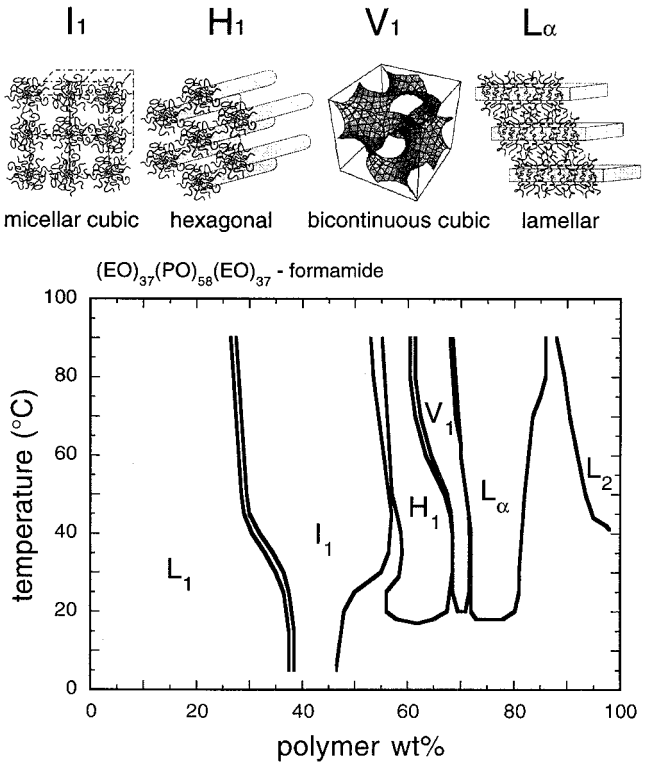

Figure 1. The concentration−temperature phase diagram of the $(EO)_{37}(PO)_{58}(EO)_{37}$−formamide binary system. The concentrations are expressed in wt %. The phase boundaries of the one-phase regions are drawn with solid lines. I_1, H_1, V_1, and L_α denote micellar cubic, hexagonal (cylindrical), bicontinuous cubic, and lamellar (smectic) lyotropic liquid crystalline phases, respectively, while L_1 and L_2 denote formamide-rich and polymer-rich solutions. The samples whose compositions fall outside the one-phase regions are dispersions of two different phases. The tie lines in the two-phase regions are parallel to the concentration axis (isothermal). Schematics of the different modes of self-organization of the amphiphilic block copolymers in the presence of the solvent are shown adjacent to the respective phases in the phase diagram. The *Ia*3*d*/gyroid minimal surface is used as a representation of the microstructure in the V_1 phase.

The assessment of the crystallographic space group of the cubic lyotropic liquid crystalline structures was based on the relative positions of the SAXS diffraction peaks as well as their relative intensity.[15,29] The indexing of the SAXS peaks to different crystallographic space groups was assessed by plotting the reciprocal spacings ($1/d_{hkl}$) of the various reflections versus $m = (h^2 + k^2 + l^2)^{1/2}$ (where h, k, and l are the Miller indices). For a valid assignment, such a plot should pass through the origin and be linear with a slope of $1/a$, where a is the cubic cell lattice parameter. A proper crystallographic indexation of the cubic structures is often hindered by the small number of reflections obtained from such samples; information obtained from other structures in the phase diagram can prove beneficial in this case.[15,29] In the micellar cubic structure, the lattice parameter (a) can be related to the block copolymer volume per molecule (v_p), interfacial area (α_p), and the volume fractions Φ_p and f, through simple geometrical arguments for the volume occupied by the N micelles (assumed spherical) that make up the unit cubic cell:

$$a = (36\pi N f^2)^{1/3} \frac{v_p}{2\Phi_p \alpha_p} \qquad (4)$$

Agreement between the α_p values thus obtained for a given N (which depends on the crystallographic space group) and the α_p values obtained in the (adjacent to the micellar cubic) hexagonal structure from eq 3, is indicative of the use of a correct N and space group. In the bicontinuous cubic structures, the identification of the crystallographic group from the SAXS peak assignment can be confirmed by comparing the α_p values in the (adjacent to the bicontinuous cubic) hexagonal and lamellar structures to the α_p values obtained from an analysis of the bicontinuous interfacial region described in terms of minimal surfaces of different crystallographic groups.[12,15]

Results and Discussion

Phase Behavior of the $(EO)_{37}(PO)_{58}(EO)_{37}$−Formamide System. The concentration−temperature phase diagram for the binary $(EO)_{37}(PO)_{58}(EO)_{37}$ (Pluronic P105)−formamide system is presented in Figure 1. The effects of temperature on the block copolymer self-assembly were explored over a wide temperature range (5−90 °C). The block copolymer molecules can self-organize in different thermodynamically stable microstructures, depending both on the polymer concentration (lyotropic behavior) and on the temperature (thermotropic behavior). A total of six different one-phase regions have been identified. Four "gel" regions with different lyotropic liquid crystalline structures have been characterized: micellar cubic (I_1), hexagonal (cylindrical) (H_1), bicontinuous cubic (V_1), and lamellar (smectic) (L_α). The arrangements of the block copolymers in the ordered structures are shown in the schematics of Figure 1. The microstructure in the two isotropic solution phases, one rich in formamide (L_1) and one rich in polymer (L_2), is not addressed here. We anticipate that, in the L_2 region, formamide is molecularly dissolved in the polymer but have not investigated this further. In the L_1 solution region, micelles are formed; we are currently in the process of assessing the concentrations and temperatures where micelles start forming (CMC and CMT) and the micelle radius.

The extensive I_1 micellar cubic gel region, with a convenient (in terms of temperature) "window" of thermoreversible liquid-to-gel transition, is an interesting feature of the $(EO)_{37}(PO)_{58}(EO)_{37}$−formamide phase diagram. Also notable is the presence of a region (V_1) with the rarely observed bicontinuous cubic structure. The progression of structure from a spherical to a cylindrical and then to a planar arrangement ($I_1 \rightarrow H_1 \rightarrow V_1 \rightarrow L_\alpha$) with increasing total polymer content is a consequence of the faster increase of the volume fraction of PPO in the system relative to the interfacial area that separates (encloses) the "apolar" PPO domains from the "polar" PEO and formamide. Note that we have not observed any of the reverse ("water-in-oil") lyotropic liquid crystalline structures (V_2, H_2, I_2); the PPO content of the copolymer is such (50%) that it does not favor such structures in the absence of an apolar solvent.[15] The tilt to the left (toward lower polymer concentrations) observed in the phase boundaries with increasing temperature is a reflection of the curvature decrease due to decreased swelling ("dehydration") of the PEO block.[29]

Micellar Cubic Structure (I_1). The I_1 region is stable over the 26−56 wt % polymer concentration range (see Figure 1). The samples in this region are stiff and optically isotropic (nonbirefringent), characteristics of a cubic lyotropic liquid crystalline gel. The location of this region in the phase diagram (between the micellar solution and the hexagonal phase—see below) suggests[15,31] that its microstructure consists of micelles that

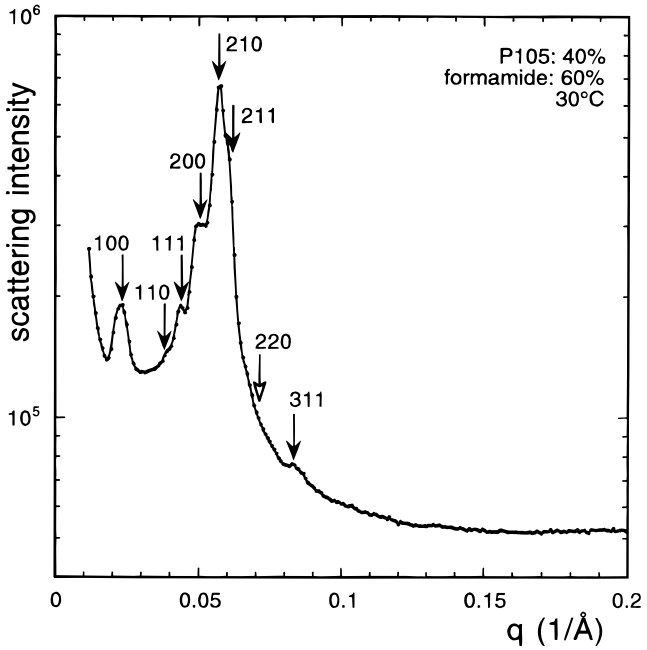

Figure 2. SAXS diffraction pattern obtained from a micellar cubic, I_1, sample of 40.0/60.0 wt % polymer/formamide (30 °C). The arrows mark the positions of the observed reflections that match the reflections afforded by the *Pm*3*n* crystallographic space group.

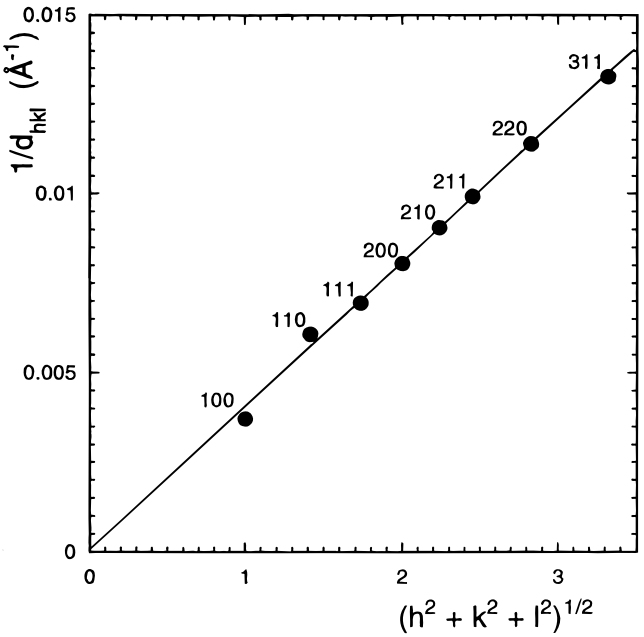

Figure 3. Reciprocal d spacings ($1/d_{hkl}$) of the reflections marked in the SAXS diffraction pattern of Figure 2 plotted versus $m = (h^2 + k^2 + l^2)^{1/2}$. The linearity of the plot and the (0,0) intercept are indications of a valid assignment to the crystallographic space group *Pm*3*n*. The micellar cubic cell lattice parameter obtained from the slope of the plot is 250 Å.

have crystallized into a cubic lattice. At temperatures below 25 °C, I_1 forms over a more limited concentration range (37−47 wt %), but at higher temperatures, I_1 extends to both lower and higher polymer contents. This is reflected in a reversible heating-induced liquid (L_1)-to-gel (I_1) transition at the 27−37 wt % and 25−45 °C ranges, reminiscent of the L_1-to-I_1 transitions observed in PEO−PPO block copolymer−water systems.[11,13] The transition from a Newtonian liquid to a soft solid material occurs in aqueous PEO−PPO block copolymer solutions when the micellar "effective" (including the solvent in the micelle coronas) volume fraction crosses the critical value for hard-sphere crystallization, for sufficiently repulsive intermicellar interactions (when the repulsion between the spherical micelles is less strong, the micelle size will increase with increasing polymer concentration and the micelles will elongate while still in solution).[11] The effective volume fraction of the PEO−PPO micelles in water increases with increasing temperature and polymer concentration and decreasing hydrostatic pressure.[11]

A SAXS diffraction pattern obtained from a I_1 sample is presented in Figure 2. A total of seven Bragg peaks were identified (marked with arrows), which can be indexed as the hkl = 100, 110, 111, 200, 210, 211, and 311 reflections of a primitive (*P*...) cubic structure. The $1/d_{hkl}$ vs $m = (h^2 + k^2 + l^2)^{1/2}$ plot shown in Figure 3 indicates the good fit of the data to the *P*... structure. The value of the cubic cell lattice parameter, a, was estimated at 250 Å from the slope of the plot of Figure 3. We note that the data can also be indexed to a body-centered *I*... structure, with a resulting lattice parameter of 350 Å. Although we have observed simple body-centered cubic structures with two micelles per unit cell before in PEO−PPO block copolymer−water systems,[15,29] the a = 250 Å value obtained here is too high for a simple primitive structure with one micelle per unit cell (and the a = 350 Å value is too high for a simple body-centered structure). So we have a more complicated structure, consisting of a number of micelles in the unit cell. A cubic structure that has often been observed with low molecular weight surfactants is that of crystallographic space group *Pm*3*n* (Q^{223}), proposed to consist of eight short (of aspect ratio 1.2−1.4) rodlike micelles per unit cell, two of then having complete rotational freedom and the other six only lateral rotational capability.[31] An alternative model suggested for the *Pm*3*n* structure involves two "quasi-spherical" and six "disk-shaped" micelles.[32] We consider the model[31] where the unit cell consists of micelles that all have the same size and shape more realistic than the model[32] involving two sets of different micelles. Note that these two models are not mutually exclusive: a short rodlike micelle revolving around its short axis (according to the model of ref 31) appears like a disklike micelle (following the model of ref 32).

Considering the (N=) 8 micelles that make up the unit cell of the *Pm*3*n* structure, and using the values of Φ_p and f for the 40.0/60.0 wt % polymer/formamide sample and the interfacial area per PEO block (assumed to be 155 Å^2 as in the H_1 sample—see below), we calculated from eq 4 a lattice parameter of 280 Å. The consistency (10% difference) of this predicted lattice parameter value with the experimentally determined one provides evidence in support of the characterization of the P105/formamide micellar cubic structure as *Pm*3*n* (an exact agreement between the experimental lattice parameter of 250 Å and that obtained from eq 4 would require α_p = 175 Å^2, a value that is reasonable given the trend of increasing α_p with decreasing polymer concentration). Moreover, the relative intensity of the peaks observed in Figure 2 follow the trend expected from the *Pm*3*n* space group.[33] From the number of micelles, N, per unit cell and the volume of the unit cell, a^3, we can obtain the volume per micelle (a^3/N), and then, given the polymer volume fraction, Φ_p, and the volume per

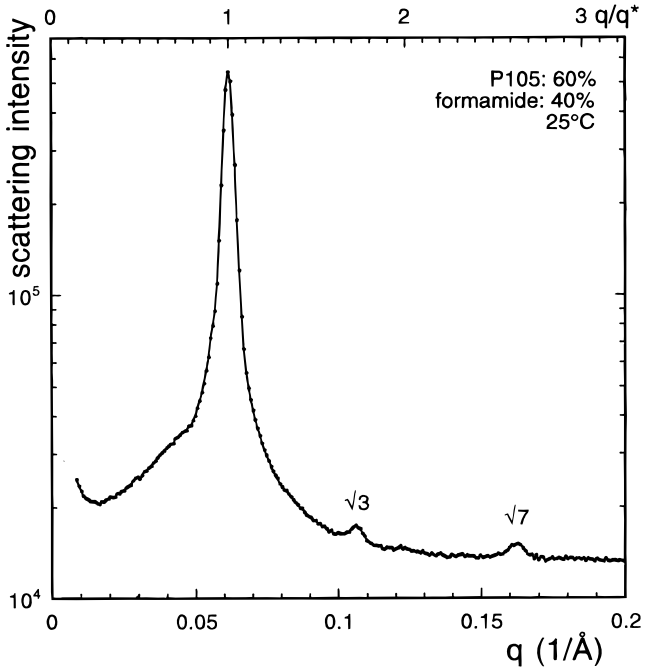

Figure 4. SAXS diffraction pattern obtained from a hexagonal, H_1, sample of 60.0/40.0 wt % polymer/formamide (25 °C). The higher order √3 and √7 Bragg peaks, characteristic of a hexagonal structure, are indicated. The positions of the higher order reflections with respect to that of the first (and most intense) peak, q^*, are indicated on the upper X-axis.

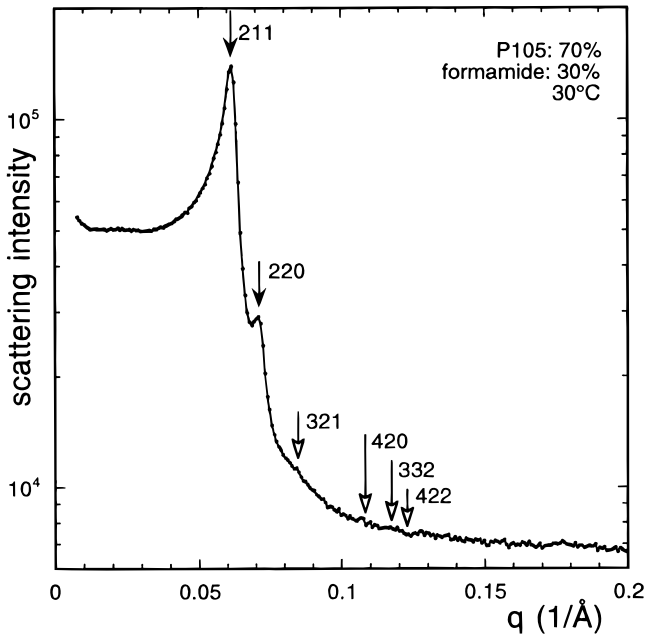

Figure 5. SAXS diffraction pattern obtained from a bicontinuous cubic, V_1, sample of 70.0/30.0 wt % polymer/formamide (30 °C). The arrows mark the positions of the observed reflections that match the reflections afforded by the *Ia*3*d* crystallographic space group.

polymer molecule, v_p, we can estimate the number of polymer molecules per micelle (association number, $N_{ass} = (\Phi_p a^3)/(N v_p)$). This value for the 40.0/60.0 wt % P105/formamide sample is 77, to be compared to the (higher) value of 157 obtained for the 40.0/60.0 wt % P105/water sample of simple body-centered cubic structure (and lattice parameter 200 Å) reported in ref 29. Although we found the P105 block copolymer to form a body-centered cubic structure in water,[29] we observed a primitive cubic structure in mixtures of P105 with a lower molecular weight PEO−PPO block copolymer (Pluronic L64: $EO_{13}PO_{30}EO_{13}$).[34] More recently, we have observed a *Pm*3*n* structure in the binary $EO_{27}PO_{61}$-EO_{27} (Pluronic P104)−water system.[35]

Hexagonal Structure (H_1). The H_1 region is stable in the 55−68 wt % polymer range (Figure 1). The concentration stability range of the H_1 region shifts from 60 to 68 wt % at 30 °C to 55−62 wt % at 70 °C (i.e., lower concentrations at higher temperatures). The two-dimensional hexagonal structure (consisting of cylindrical self-assemblies crystallized in an hexagonal lattice, as shown schematically in Figure 1) of samples in the H_1 region was established by SAXS experiments (the relative positions of the three peaks resolved in the diffraction pattern of Figure 4 follow the 1:√3:√7 relationship; the peak at position 2 is missing, for reasons that are not clear to us at this time). The nearest neighbor (cylinder) distance is 117 Å at 60.0/40.0 wt % polymer/formamide. The area per PEO block at the interface enclosing the cylindrical PPO domains (of radius 34 Å) is 155 Å^2. These values are to be compared to a = 140 Å, α_p = 130 Å^2, and R = 41 Å obtained in the P105−water system at the same composition and temperature.[29] Thus, the cylindrical assemblies in the P105−formamide system are more closely packed and more numerous than in P105−water.

Bicontinuous Cubic Structure (V_1). The V_1 region occurs in the 61−72 wt % polymer concentration range (Figure 1). It starts off at 20 °C, centered at 70 wt % polymer and narrow, but at higher temperatures it swells with formamide (to the expense of the H_1 structure) and extends over the 62−68 wt % range. The samples in the V_1 region are optically isotropic (nonbirefringent) and very stiff, characteristics of cubic structure; the location of this cubic region in the phase diagram (between regions of H_1 and L_α structure) indicates that the structure in V_1 is bicontinuous with the curvature of the polar/apolar interface toward the apolar PPO.[15,31] Two complementary descriptions are used for bicontinuous cubic phases in surfactant and block copolymer systems: (i) a multiply connected bilayer (described in terms of minimal surfaces of cubic symmetry) separating two distinguishable and continuous domains of the same solvent and (ii) two infinite channel networks of interconnected cylinders (associated with the skeletal graphs of the two interwoven subvolumes separated by the minimal dividing surface of the bilayer description).[12,15,36] We can thus visualize the microstructure in the V_1 region to be that of a polar film consisting of PEO and formamide, which forms a dividing layer between two apolar domains containing PPO (as shown in the schematic of Figure 1 and, with better resolution, in Figure 10a of ref 36).

A SAXS diffraction pattern obtained from a sample in the V_1 region is shown in Figure 5. The scattering function in Figure 5 is dominated by a strong correlation peak at q = 0.0616 Å^{-1}. The most commonly observed space group of bicontinuous cubic phases in surfactant and lipid systems is *Ia*3*d* (Q^{230}),[15,31] where the bilayer/channel structure can be associated with the so-called gyroid (G) minimal surface. This space group allows the Bragg reflections hkl = 211, 220, 321, 400, 420, 332, 422, ... which give rise to peaks in the relative scattering vector positions √6, √8, √14, √16, √20, √22, √24, ...[33] The first reflection, corresponding to hkl = 211, is

the most intense.[33] The second well-defined reflection in the diffraction pattern of Figure 5 follows the sequence $1:\sqrt{8}/\sqrt{6}$ (=1.155) with respect to the first peak (hkl = 211) and is hence consistent with the 220 reflection of the $Ia3d$ space group; a number of other (weak) peaks are marked in the SAXS diffraction pattern of Figure 5 with arrows and can be identified as the higher order (321, 420, 332, and 422) reflections of the $Ia3d$ structure. From the linear fit of the $1/d_{hkl}$ vs $m = (h^2 + k^2 + l^2)^{1/2}$ plot, we obtained a cell lattice parameter value for the V_1 structure of a = 250 Å.

The presence of the bicontinuous cubic structure is a notable feature of the $(EO)_{37}(PO)_{58}(EO)_{37}$−formamide phase diagram. Bicontinuous cubic phases were first identified in lipid−water and surfactant−water systems in the 60s.[31] The appeal of such phases increased when their microstructure was related to a geometrical description based on minimal surfaces.[37] Bicontinuous cubic phases of the $Ia3d$/gyroid structure have been observed in solvent-free block copolymers.[3,38] We have reported the formation of such structures (but of the reverse "water-in-oil" topology, where an apolar PPO + oil film forms a dividing layer between two polar PEO + water domains) in ternary amphiphilic di- and triblock copolymer−water−oil systems.[12,15,35,36,39] There is only a single report of a ("oil-in-water") bicontinuous cubic structure in a binary PEO−PPO block copolymer−water system.[15] Such complex structures hold intriguing implications in processes involving biological membranes (e.g., fusion)[37] and can be used as templates for, e.g., the synthesis of porous membranes with well-defined structure and pore size (by the polymerization of a macromonomer-amphiphile or a monomer acting as solvent).[40] The use of formamide as a solvent may increase the possible routes for the synthesis of such material.

Lamellar Structure (L_α). The L_α region extends from 68 to 86 wt % polymer at temperatures above 70 °C and from 72 to 82 wt % polymer at temperatures of 20−50 °C (Figure 1). The one-dimensional lamellar (smectic) structure (shown schematically in Figure 1) of the samples in the L_α region has been established by SAXS measurements that gave diffraction patterns with second-order peaks obeying the 1:2 relationship (as seen in Figure 6). The values for the lamellar periodicity (lattice spacing), d, the apolar (PPO) thickness, δ, and the interfacial area per PEO block, α_p, are 101, 40, and 135 Å^2, respectively, at 75.0/25.0 wt % polymer/formamide. In water, and at the same composition and temperature, P105 exhibits a lamellar periodicity of 114 Å and interfacial area of 120 Å^2. The difference in a and α_p between the formamide and the water systems is smaller in the lamellar region than in the hexagonal region (≈10% difference in the lamellar region vs ≈20% difference in the hexagonal). The trend of lower lamellar periodicity in the P105−formamide system compared to the P105−water is similar to what has been observed in a nonionic PEO−alkyl ether surfactant ($C_{16}EO_4$).[23]

Formamide vs Water-Phase Behavior and Microstructure. We have previously reported[29] the binary $(EO)_{37}(PO)_{58}(EO)_{37}$−water ($^2H_2O$) concentration−temperature phase diagram, and we present this phase diagram here (Figure 7) in order to compare it (at the same coordinates and notation) to the $(EO)_{37}(PO)_{58}$-$(EO)_{37}$−formamide system. Inspection of the formamide and water phase diagrams can give us a "bird's eye" view of the solvent effects on the block copolymer

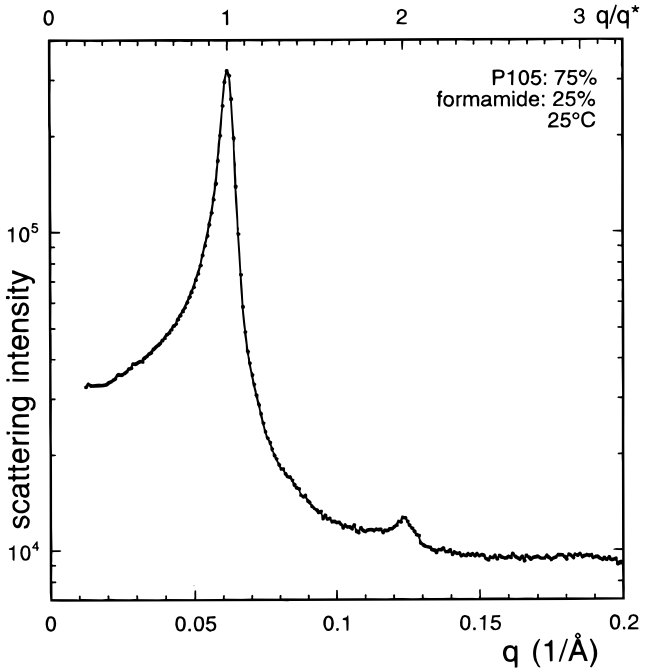

Figure 6. SAXS diffraction pattern obtained from a lamellar, L_α, sample of 75.0/25.0 wt % polymer/formamide (25 °C). The positions of the higher order reflections with respect to that of the first (and most intense) peak, q^*, are indicated on the upper X-axis.

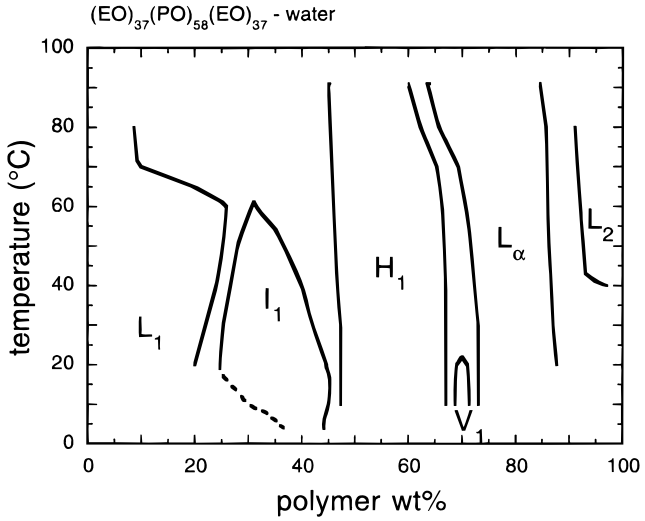

Figure 7. Concentration−temperature phase diagram of the $(EO)_{37}(PO)_{58}(EO)_{37}$−water ($^2H_2O$) binary system (adapted from ref 29). The concentrations are expressed in wt %. The notation is the same as in Figure 1.

microstructure, whereas the structural parameters extracted from SAXS using eqs 1−4 provide a more "microscopic" view. As discussed below, a consistent picture emerges from both phase behavior and structure in terms of what are the effects of formamide on self-assembly.

The following general observations can be made from the phase diagrams: (i) the structural polymorphism of the PEO−PPO block copolymer is not diminished by having formamide as a selective solvent instead of water, (ii) the stability regions of all the "curved" (nonlamellar) structures (and in particular of the micellar cubic I_1 region) are shifted to higher polymer concentrations and temperatures in the case of form-

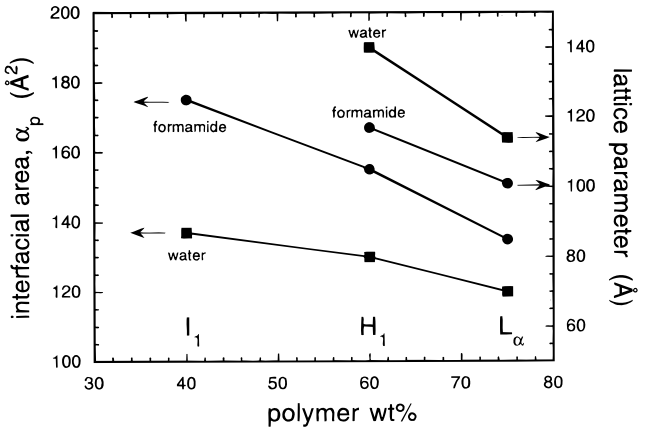

Figure 8. Lattice parameters, *d*, in the hexagonal and lamellar structures and interfacial area-per-polymer values, α_p, in the micellar cubic, hexagonal, and lamellar structures plotted as a function of the polymer wt % both for the $(EO)_{37}(PO)_{58}(EO)_{37}$−formamide and for the $(EO)_{37}(PO)_{58}(EO)_{37}$−water binary systems.

amide compared to water, and (iii) the bicontinuous cubic V_1 region, usually very rare and very narrow,[12,15] is stable with formamide as solvent, and even wins over the H_1 structure at higher temperatures (the H_1 region in formamide is stable over a concentration range narrower than that in water).

On the basis of the SAXS structural data, we can conclude that (iv) the structural elements (micelles) of the I_1 cubic structure in formamide are much smaller (and possibly ellipsoidal) than those in water and (v) the lattice parameters in the lamellar and hexagonal structures are 10% and 20% lower, respectively, in formamide than in water (the structural elements are more and closer together in formamide), and the corresponding interfacial area-per-polymer values are 10% and 20% higher, respectively, in formamide compared to water. The above trends are depicted in Figure 8, where the lattice parameters in the hexagonal and lamellar structures and the interfacial area-per-polymer values in the micellar cubic, hexagonal and lamellar structures are plotted as a function of the polymer wt % both for the $(EO)_{37}(PO)_{58}(EO)_{37}$−formamide and for the $(EO)_{37}(PO)_{58}(EO)_{37}$−water binary systems.

(i) We chose to study $(EO)_{37}(PO)_{58}(EO)_{37}$ in formamide because we knew[29] that this polymer forms a number of different structures (having different temperature stabilities) in water and wanted to examine their fate in the presence of a different solvent. Lyotropic liquid crystalline phases are formed in surfactant−formamide systems, but generally, for such structures to form, surfactants with longer hydrophobic parts are required as compared to the case with water[25] (e.g., 16 methyl segments, C, for formamide instead of 12 C for water, in the case of nonionic PEO-alkyl ether surfactants[23]). Furthermore, the stability of some of the structures decreases in the presence of formamide (e.g., the $C_{16}EO_8$−water system exhibits I_1, H_1, V_1, and L_α structures,[30] whereas the $C_{16}EO_8$−formamide system only H_1[23]). The fact that all the structures observed in the PEO−PPO block copolymer−water system are maintained in formamide shows that the tendency of these block copolymers to segregate and form ordered structures at concentrations above ≈30 wt % is strong and is not diminished by the solvent−PPO interaction, which is weaker in formamide than in water.

(ii) The shift of the stability regions of the L_1 and I_1 structures formed in formamide to higher (compared to water) polymer concentrations and temperatures can be related to high CMC/CMT (microphase separation; affected by the formamide−PPO interaction parameter χ_{fm-PPO}) of the PEO−PPO block copolymer in formamide. The CMCs of nonionic PEO−alkyl ether surfactants in formamide are 100−1000 times higher than those in water.[22] High CMC/CMT do not inhibit the formation of a micellar cubic structure. For example, the CMC of Pluronic P105 in water is 0.001% at 40 °C and the micellar cubic gel is formed at ≈30%,[8] while Pluronic F68, of comparable molecular weight (8400) and much higher PEO content (80%), has a CMC in water of 7% at 40 °C and still forms a micellar cubic phase at concentrations ≈40%.[13] The much higher temperature stability range of the I_1 structure in formamide is also connected to the higher solubility of the PEO−PPO block copolymer in formamide as reflected in the cloud point (macrophase separation into polymer-rich and a solvent-rich solutions because of limited solubility of the polymer in the solvent; affected by the formamide−PEO interaction parameter χ_{fm-PEO}) which is ≈50 °C higher in formamide than the cloud point in water.[26] The "melting" of the $(EO)_{37}(PO)_{58}(EO)_{37}$ I_1 cubic structure in water at ≈60 °C corresponds to the cloud point of the polymer.[29]

(iii) The finding of a bicontinuous cubic region in the $(EO)_{37}(PO)_{58}(EO)_{37}$−formamide system was particularly enticing because such a structure had not been observed in water.[29] It turned out upon revisiting the $(EO)_{37}(PO)_{58}(EO)_{37}$−water system, that a V_1 structure is indeed formed in water at ≈70 wt % polymer but is stable over a very narrow concentration range and below 20 °C (the lower temperature studied in the phase diagram of ref 29). As to the reasons behind the stability of the bicontinuous cubic structure in formamide, one possibility is fluctuation effects (presumably more important in formamide than in water, especially if some formamide is also located in the PPO regions—see paragraph v). The stability of bicontinuous cubic phases localized near the order−disorder transition (ODT) in diblock copolymer melts has been related to fluctuation effects that favor isotropic (such as bicontinuous cubic) microstructures.[41] It is notable that growth of V_1 (to the expense of H_1) has also been observed in various surfactant−formamide systems.[42]

(iv) The smaller micelles (association number 77 compared to 157 in water) participating in the I_1 cubic structure in formamide (consistent with observations in micellar solution of nonionic surfactants[22]) are an indication of weaker formamide−PPO interactions (χ_{fm-PPO} smaller than $\chi_{water-PPO}$), the consequences of which can be represented by the polymer having an effective PEO/PPO block ratio higher in formamide than in water. Small micelles expose a larger part of the PPO chains to the solvent, but if the formamide−PPO interactions are weak, the enthalpic penalty for this is low.

(v) The higher interfacial area per block copolymer in the formamide system (Figure 8) indicates that the polymer molecules are more swollen by the solvent than in water (consistent with the observation of increasing interfacial area with increasing solvent content from L_α to H_1) and/or an increase in the effective PEO/PPO block ratio. If we take the area per molecule (120 Å^2) in the P105−water lamellar region as a basis, then in order

to obtain (from eq 3) the same area in formamide we need to assume that some formamide participates in the interfacial volume fraction (in excess of the block copolymer volume fraction Φ_p).[17] In the hexagonal structure, an area consistent with that in water can be obtained by either increasing Φ_p or decreasing the apolar volume fraction f (eq 3).

Summary

We established the binary concentration−temperature phase diagram and the microstructure of a poly(ethylene oxide)−poly(propylene oxide) (PEO−PPO) block copolymer (Pluronic P105: $EO_{37}PO_{58}EO_{37}$) in formamide (as selective solvent for PEO.

The block copolymer molecules can self-assemble in six different thermodynamically stable microstructures, exhibiting both lyotropic and thermotropic behavior. A thermoreversible transition from a micellar solution to a micellar cubic gel occurs at 25−35 wt % polymer concentrations. At higher concentrations, regions with hexagonal (cylindrical), bicontinuous cubic, and lamellar (smectic) lyotropic liquid crystalline structures are stable. The crystallographic structure of the micellar and bicontinuous cubic samples is found, consistent with the *Pm*3*n* and *Ia*3*d*/gyroid space groups, respectively.

The stability regions of the different structures (and in particular of the micellar cubic) in the case of formamide are shifted to higher polymer concentrations and temperatures compared to water, suggesting that the effective curvature of the interfaces formed by the block copolymer is higher in formamide than in water. Indeed, the interfacial area-per-polymer values in the lamellar and hexagonal structures are 10% and 20% higher, respectively, in the case of formamide than in water. Also, the number of block copolymer molecules participating in each micelle in the formamide micellar cubic gel is half that in water.

These observations can be rationalized in terms of a higher solubility of both PEO and PPO in formamide compared to water (χ_{fm-PPO} and χ_{fm-PEO} lower than $\chi_{water-PPO}$ and $\chi_{water-PEO}$, respectively), and a higher effective PEO/PPO block ratio of the copolymer. The determination of the concentrations and temperatures where micelles start forming (CMC and CMT), currently in progress in our laboratory, will provide[8] the thermodynamic parameters of micellization (free energy, $\Delta G°$, enthalpy, $\Delta H°$, and entropy, $\Delta S°$) and offer more quantitative information on the PPO−formamide and PEO−formamide interactions.

Acknowledgment. The experiments described in this paper were carried out at Physical Chemistry 1, Center for Chemistry and Chemical Engineering, Lund University, Sweden, and were supported financially by the Swedish Natural Science Research Council (NFR). The laboratory assistance of Karin Andersson is appreciated. Discussions with Professor R. Strey (University of Cologne, Germany) stimulated us to pursue this investigation.

References and Notes

(1) Evans, D. F.; Wennerström, H. *The Colloidal Domain: Where Physics, Chemistry, Biology, and Technology Meet*; VCH Publishers: New York, 1994.
(2) Laughlin, R. G. *The Aqueous Phase Behavior of Surfactants*; Academic Press: London, 1994.
(3) Bates, F. S. *Science* **1991**, *251*, 898−905. Lohse, D. J.; Hadjichristidis, N. *Curr. Opin. Colloid Interface Sci.* **1997**, *2*, 171−176.
(4) Moffitt, M.; Khougaz, K.; Eisenberg, A. *Acc. Chem. Res.* **1996**, *29*, 95−102.
(5) Alexandridis, P. *Curr. Opin. Colloid Interface Sci.* **1996**, *1*, 490−501.
(6) Förster, S.; Antonietti, M. *Adv. Mater.* **1998**, *10*, 195−217.
(7) Alexandridis, P. *Curr. Opin. Colloid Interface Sci.* **1997**, *2*, 478−489.
(8) Alexandridis, P.; Holzwarth, J. F.; Hatton, T. A. *Macromolecules* **1994**, *27*, 2414−2425.
(9) Schmolka, I. R. *J. Am. Oil Chem. Soc.* **1991**, *68*, 206−209.
(10) Paavola, A.; Yliruusi, J.; Rosenberg, P. *J. Controlled Release* **1998**, *52*, 169−178.
(11) Mortensen, K. *J. Phys.: Condens. Matter* **1996**, *8*, A103-A124.
(12) Alexandridis, P.; Olsson, U.; Lindman, B. *Macromolecules* **1995**, *28*, 7700−7710.
(13) Wanka, G.; Hoffmann, H.; Ulbricht, W. *Macromolecules* **1994**, *27*, 4145−4159.
(14) Chu, B. *Langmuir* **1995**, *11*, 414−421.
(15) Alexandridis, P.; Olsson, U.; Lindman, B. *Langmuir* **1998**, *14*, 2627−2638.
(16) De Gennes, P. G. *Solid State Phys. Suppl.* **1978**, *14*, 1−18.
(17) Holmqvist, P.; Alexandridis, P.; Lindman, B. *Macromolecules* **1997**, *30*, 6788−6797.
(18) Cheng, Y.; Jolicoeur, C. *Macromolecules* **1995**, *28*, 2665−2672.
(19) Alexandridis, P.; Holzwarth, J. F. *Langmuir* **1997**, *13*, 6074−6082.
(20) Evans, D. F. *Langmuir* **1988**, *4*, 3−12.
(21) Ellis, B. N. *Cleaning and Contamination of Electronic Components and Assemblies*; Electrochemical Publication, Ltd.: Essex, U.K., 1986.
(22) Wärnheim, T. *Curr. Opin. Colloid Interface Sci.* **1997**, *2*, 472−477.
(23) Jonströmer, M.; Sjöberg, M.; Wärnheim, T. *J. Phys. Chem.* **1990**, *94*, 7449−7555.
(24) Ceglie, A.; Colafemmina, G.; Della Monica, M.; Olsson, U.; Jönsson, B. *Langmuir* **1993**, *9*, 1449−1455.
(25) Schubert, K. V.; Busse, G.; Strey, R.; Kahlweit, M. *J. Phys. Chem.* **1993**, *97*, 248−254.
(26) Samii, A. A.; Karlström, G.; Lindman, B. *Langmuir* **1991**, *7*, 1067−1071.
(27) Imhof, A.; Pine, D. J. *Nature* **1997**, *389*, 948−951.
(28) Alexandridis, P.; Athanassiou, V.; Hatton, T. A. *Langmuir* **1995**, *11*, 2442−2450.
(29) Alexandridis, P.; Zhou, D.; Khan, A. *Langmuir* **1996**, *12*, 2690−2700.
(30) Mitchell, J. D.; Tiddy, G. J. T.; Waring, L.; Bostock, T.; McDonald, M. P. *J. Chem. Soc., Faraday Trans. 1* **1983**, *79*, 975−1000.
(31) Fontell, K. *Colloid Polym. Sci.* **1990**, *268*, 264−285.
(32) Vargas, R.; Mariani, P.; Gulik, A.; Luzzati, V. *J. Mol. Biol.* **1992**, *225*, 137−145.
(33) Mariani, P.; Luzzati, V.; Delacroix, H. *J. Mol. Biol.* **1988**, *204*, 165−189.
(34) Zhou, D.; Alexandridis, P.; Khan, A. *J. Colloid Interface Sci.* **1996**, *183*, 339−350.
(35) Svensson, B.; Alexandridis, P.; Olsson, U. *J. Phys. Chem. B.* **1998**, *102*, 7541.
(36) Alexandridis, P.; Olsson, U.; Lindman, B. *Langmuir* **1997**, *13*, 23−34.
(37) Hyde, S.; Andersson, S.; Larsson, K.; Blum, Z.; Landh, T.; Lidin, S.; Ninham, B. W. *The Language of Shape − The Role of Curvature in Condensed Matter: Physics, Chemistry and Biology*; Elsevier Science B.V.: Amsterdam, 1997.
(38) Avgeropoulos, A.; Dair, B. J.; Hadjichristidis, N.; Thomas, E. L. *Macromolecules* **1997**, *30*, 5634 and references therein.
(39) Alexandridis, P.; Olsson, U.; Lindman, B. *J. Phys. Chem.* **1996**, *100*, 280−288.
(40) Lee, Y.-S.; Yang, J.-Y.; Sisson, T. M.; Frenkel, D. A. Gleeson, J. T.; Aksay, E.; Keller, S. L.; Gruner, S. M.; O'Brien, D. F. *J. Am. Chem. Soc.* **1995**, *117*, 5573−5578.
(41) Bates, F. S.; Schulz, M. F.; Khandpur, A. K.; Förster, S.; Rosedale, J. H.; Almdal, K.; Mortensen, K. *Faraday Discuss.* **1994**, *98*, 7−18.
(42) Sjöberg, M.; Wärnheim, T. *Surfactant Sci. Ser.* **1997**, *67*, 179−205.

MA9807522